Transient Pressure Analysis and Air-water Interaction in Churn Flow

H.-J. Lin, M.-S. Lin, P.-S. Ruan, S.-W. Chen, J.-D. Lee, and J.-R. Wang

***Abstract*—In this study, normal scale air-water two-phase flow experiments and a new method were carried out to identify the momentum characteristic of churn flow pattern. To acquire proper and sufficient information for the complicated flow pattern, narrow differential pressure (NDP) and conductivity probes signals were measured simultaneously and analyzed. The experiments were performed under the conditions whose superficial gas velocity (Jg) and the superficial fluid velocity (Jf) were 6.28 m/s and 0.0236-0.9912 m/s, respectively. Through visualization and pressure signals analysis, the air-water interaction of churn flow could be categorized into two types: Helmholtz type and disperse type. The diverse characteristics and various combination ratios of these two types of different air-water interaction are the reasons that make churn flow a more complex regime than the others. Through signal separation methods, the quantified characteristics of each type as well as the variation originated from flow rate changing of these two air-water interaction could be revealed.**

***Index Terms*—Air-water two-phase flow, churn flow, momentum characteristic, pressure signals, visualization, transient signal analysis.**

I. Introduction

Two-phase flow is widely used in many industrial applications, for example, nuclear reactor and oil transportation. In general, the flow regimes are determined by varieties of parameters, such as velocity, temperature, pressure drop, as well as flow channel size and geometry. The flow patterns of two-phase flow in an upward vertical pipe could be categorized into several flow regimes, like bubbly flow, slug flow, churn flow and annular flow etc. [1], [2]. Every flow regime has its own quite different characteristic and physical phenomena, for example, air-water volume ratio, momentum characteristics and heat transfer characteristics. Hence, how to identify the flow regimes accurately and efficiently is always an important issue. The identification of two-phase flow regimes is utilized to describe the behaviors of each flow regimes and predict under specific operating conditions. The flow regimes are identified from flow-regime maps which have been proposed based on the liquid and gas superficial velocity obtained from experimental observations. Fig. 1 shows the schematics of the two-phase flow patterns in an upward tube, and the flow regimes from left to right normally represent the gas flow rate from lower to higher under a constant liquid flow condition.

Among the above mentioned flow a regime, churn flow had long been considered as the transition between slug flow and annular flow. Comparing to other flow patterns, fewer researches about churn flow have been done. However, the complexity of air-water interaction in churn flow, like entrainments and depositions [4], [5] can trigger the instability of the system. This may cause some concerns on nuclear safety. In the past, most researchers mainly used void fraction to conduct researches, which could only reveal little information about air-water interaction. Pressure signals, on the other hand, can respond to the variation of velocity and acceleration of liquid. This can tell us a lot of information about air-water interaction regarding momentum characteristics. In this study we mainly use pressure signals and high frame rate photos to identify detailed air-water interaction in churn flow.

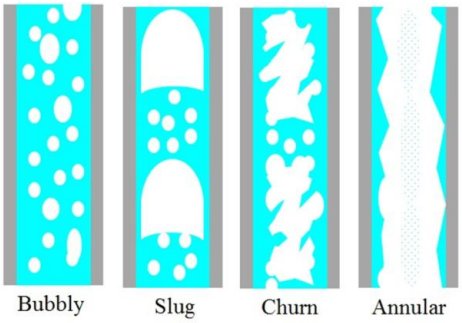

Fig. 1. The flow patterns of two-phase flow in vertical pipe [3].

II. Experimental Facility

In this study, an upward air-water two-phase flow facility was constructed and tested for churn and annular flow liquid layer thickness characteristics. Fig. 2 shows the schematic of the two-phase flow experimental devices for the present study, including test section, buffer region, water supply system (water pump, tank, bypass valve, etc.), air supply systems (air compressor, air tank, control valve, etc.), instruments (air/water flow meters, pressure sensors, high frame rate camera, etc.) and data acquisition system, etc.

The test section was made of acrylic circular tube with 3.0 cm inside diameter, and the total length of the test section is five-meters height. It was remained about 50 cm length for the buffer region before water tank (4.5m~5.0m), and the developing region (0~2.5m) is the first parts of test section. The following is measurement region (2.5m~4.0m) and the visualization region (4.0m~4.5m). For the water supply system, it consists of a high-pressure 3-HP water pump, a set of two-level water flow meter, flow control valves and bypass valve/line. Compressed air and water were pumped into the mixer and flowed into the test section. The air supply system consists of a 5HP-compressor, 304L-air tank, a set of three-level air flow meters, flow control valves and a pressure regulator, and the air tank was maintained at a pressure of

Manuscript received July 19, 2018; revised August 30, 2018.

The authors are with National Tsing Hua University, Taiwan (e-mail: zody1994@gmail.com).

73.5 psig by the pressure regulator for continuous air supply to the mixer and test section. Table I shows the specification of the flow meters of the present study. The measurement region includes the three pressure sensors (for multi-range differential pressure measurement) and electric conductivity sensors (for void fraction measurement). Table II shows the specification of the pressure and conductivity sensors of the present study.

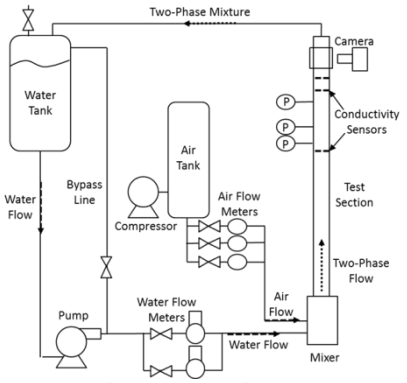

Fig. 2. The schematic of the two-phase flow experimental devices.

TABLE I: THE SPECIFICATIONS OF THE FLOW METERS

Flow Meters	Range (Liter/min)		Precision
	Min	Max	(full scale)
High flow (Air)	60	600	±1%
Mid flow (Air)	10	100	±1%
Low flow (Air)	1	20	±1%
High flow (Water)	20	300	±1%
Low flow (Water)	1	20	±1%

TABLE II: THE SPECIFICATIONS OF THE PRESSURE/CONDUCTIVITY SENSORS

Pressure/Cond. Sensors	Range	Sensitivity	Frequency Response (Hz)
Wide-range DP (80cm)	15.00 psig	1/1000	0~1k
Narrow-range DP (10cm)	1.00 psig	1/1000	0~1k
Gauge Pressure	15.00 psig	1/1000	0~1k
Conductivity Sensors	0-10V	1/1000	0~100k

The schematic of conductivity sensors is shown in the left-down portion of Fig. 3, which were made of two copper circular plates (length= 1mm) inserted in the pipe inner wall (totally fitted the original ID without perceptible steps). The measuring mechanism of conductivity sensors for void fraction was very similar to the impedance void meters utilized in reference [6], [7]. The DC circuit was used in the present experiment which stabilize signal. After calibrations, the compound uncertainty of the conductivity sensors for void fraction measurement can be controlled about 5%. During the experiments, the transient signals of void fraction may vary rapidly; hence the operating frequency of data acquisition was set as about 4000-10000Hz during the experiments.

At the upper part of the test section (about 420 cm heights), a view port of visualization region was constructed with a transparent water box surrounding the test section to avoid image distortion by deflection. Moreover, the data acquisition system adopts an industrial personal computer and A/D cards to acquire analog voltage signals from conductivity and pressure sensors. Then the Matlab programs were used to convert these signals into pressure and void fraction values for the present study.

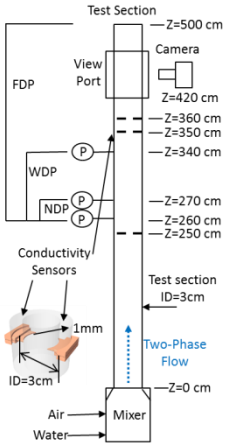

Fig. 3. The schematic of pressure sensors.

III. RESEARCH METHODS

A. Pressure Loss

Total pressure loss in a vertical circular pipe can be showed like (1):

$$\Delta P_{\text{total}} = \Delta P_{\text{friction}} + \Delta P_{\text{acceleration}} + \Delta P_{\text{gravitation}} \quad (1)$$

During an adiabatic and isothermal process, the expansion of gas phase can be neglected. Then the total pressure loss becomes (2):

$$\Delta P_{\text{total}} = \Delta P_{\text{friction}} + \Delta P_{\text{gravitation}} \quad (2)$$

The pressure loss of gravity is (3)

$$\Delta P_{\text{gravitation}} = \rho_f g(1-\alpha)\text{L}+\rho_g g\alpha\text{L} \quad (3)$$

where L is length of pipe and g is gravitational acceleration. Density of water is extremely larger than gas ($\rho_f \gg \rho_g$), so the term of gas phase is neglected like equation (4):

$$\Delta P_{\text{gravitation}} = \rho_f g(1-\alpha)\text{L} \quad (4)$$

The pressure loss term of friction is derived from Blasius friction pressure loss equation (5)

$$\Delta P_{fric} = \frac{C_{fric}}{D}\frac{G^2}{2\rho_f g}\Phi_{\ell 0}^2 \quad (5)$$

where D、G、C_{fric} and $\Phi_{\ell 0}^2$ are diameter of pipe, mass, flux, friction factor and two-phase multiplier, respectively.

From equation (4) and (5), the total pressure loss can be showed (6)

$$\Delta P_{\text{total}} = \frac{C_{fric}}{D}\frac{G^2}{2\rho_f g}\Phi_{\ell 0}^2 + \rho_f g(1-\alpha)\text{L}+\rho_g g\alpha\text{L} \quad (6)$$

B. Void Fraction

Maxwell (1881) equation is used to do the estimation of void fraction in the present study, and the equation is showed below:

$$\alpha_G = \left[\frac{A-A_C}{A+2A_C}\right]\left[\frac{C_G+2C_L}{C_G-C_L}\right] \quad (7)$$

where A_C is the admittance of the gauge system when immersed in the liquid phase alone. C_G and C_L are the gas and liquid conductivities. Because C_G and C_L have a large difference, C_G is assumed to approximate zero. Then the equation becomes:

$$\alpha_G = -2\left[\frac{A-A_C}{A+2A_C}\right] \quad (8)$$

The similar method as Maxwell equation (dimensionless voltage) was utilized to measure void or liquid fraction in the past study. Maxwell equation has a great performance for the estimation of void fraction.

IV. Results and Discussion

Typically, churn flow is composed of looping deformed Taylor bubbles and disperse mixture sections. The dynamic air-water interaction of the both two flow patterns can lead to pressure impulses. Through visualization we found that they have distinct characteristics. Pressure impulses caused by Helmholtz waves in deformed Taylor bubbles is called Helmholtz Type. On the other hand, pressure impulses caused by dispersed mixture section is called disperse type.

A. Two Types of Air-Water Interaction

Helmholtz Types are occurred in deformed Taylor bubbles. When Helmholtz waves crash with liquid entrainments, a series of liquid entrainments and depositions would be re-created. This active air-water interaction is the reason why the pressure impulses of Helmholtz types can be created even with relatively small liquid fraction. Figs. 4-5 show the schematic and visualization of Helmholtz type. Fig. 6 shows the pressure impulses after signal separation procedure.

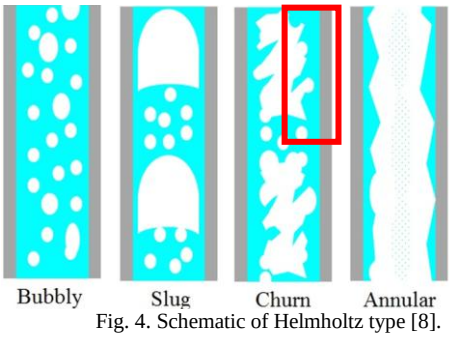

Fig. 4. Schematic of Helmholtz type [8].

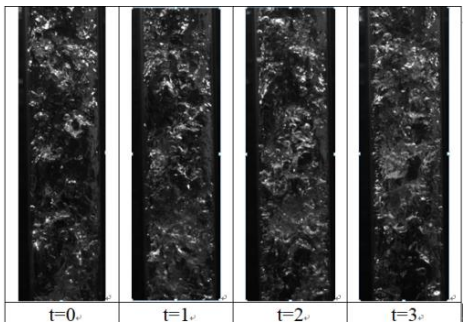

Fig. 5. Visualization of Helmholtz type [8].

Disperse type pressure impulses occur when low velocity deformed Taylor bubbles sections are taken place by high velocity disperse mixture sections. Due to the velocity variation between two sections, the liquid would be accelerated therefore cause pressure signal impulses. Comparing to Helmholtz type, disperse type has higher pressure difference value with higher liquid fraction. Fig. 7-8 shows the schematic and visualization of disperse type. Fig. 9 shows the pressure impulses after signal separation procedure.

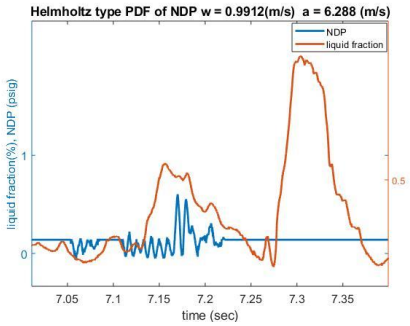

Fig. 6 Helmholtz type pressure impulse

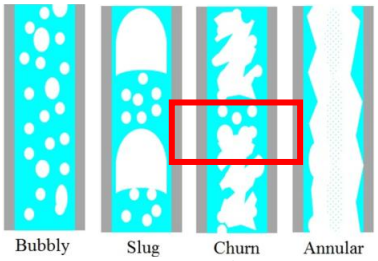

Fig. 7. Schematic of disperse type [8]

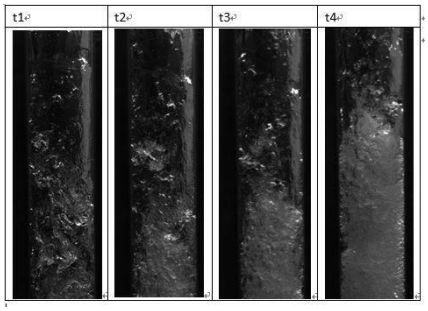

Fig. 8. Visualization of disperse type [8].

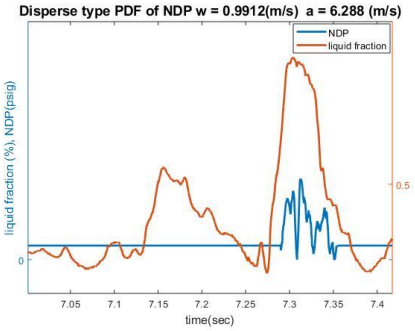

Fig. 9. Disperse type pressure impulse.

B. Comparison and Further Analysis of Two Air-Water Interaction Types

By comparing NDP PDF diagrams with different flow conditions of both types (like Fig. 10), we found that the NDP PDF of disperse type are wider than Helmholtz type's. This is because disperse type generally has fiercer air-water interaction than the Helmholtz type's. For example, crashes between large downward liquid chunks at liquid film and

upward air-water mixture sections. These would cause more transient and fierce fluctuations during the pressure impulses. This is the reason why the NDP PDF of disperse type are wider than Helmholtz type's. Moreover, we also found that due to the typically higher liquid velocity of disperse type, the NDP PDF of disperse type have larger chunk on high pressure region and higher PDF centroids than the Helmholtz type's.

The NDP PDF diagrams of each type and their variations with different flow conditions have also been compared. It was found that the maximum pressure value of each type would increase as fluid velocity increased; however, only the portions of high pressure region of disperse type's NDP PDF would increase as fluid velocity increased.

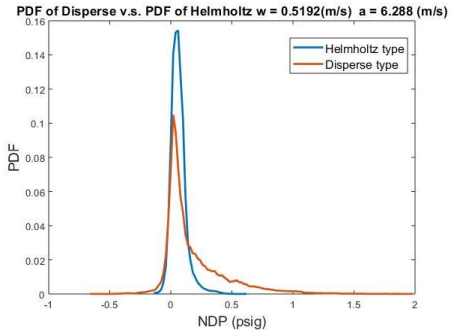

Fig. 10. The comparison of NDP PDF between two types at *Jl*=0.5192 m/s, *Jv*=6.288 m/s.

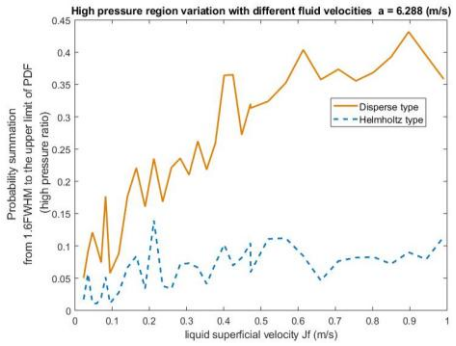

Fig. 11. The comparison of high pressure portion of NDP PDF.

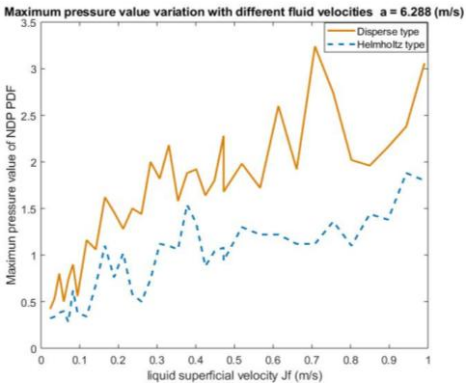

Fig. 12. The comparison of maximum pressure value of NDP PDF.

We also compared each type's variations with different flow conditions. Fig. 11 shows the portion of high pressure region variation of each type with different flow conditions. Fig. 12 shows the maximum pressure value variation of each type with different flow conditions. We found that the maximum pressure value of each type would both increase as fluid velocity increased, However, only the portion of high pressure region in disperse type would hugely increase as fluid velocity increased.

V. Conclusion

By analyzing narrow range pressure difference (NDP) as well as observing high frame rate photos, the air-water interaction can be broken into two types: Helmholtz type and disperse type. The NDP PDF diagrams of each type and their variations with different flow conditions have been compared. It was found that the maximum pressure value of each type would increase as fluid velocity increased; however, only the portions of high pressure region of disperse type's NDP PDF would increase as fluid velocity increased. It shows that the increment of liquid velocity would not equally affect the magnitude characteristic of the both types. Disperse type is more susceptible to liquid velocity increment. One of our future works is to change air velocity under fixing liquid velocity to see the influence of gas increment on the both types.

In this study, we mainly use pressure signals to conduct our research. The merit of using pressure signals is to reveal momentum characteristics regarding air-water interaction which could not be revealed by merely using void fraction signals. This may be another effective way to identified air-water two-phase flow regimes with the consideration of momentum and air-water interaction. Therefore, one of our future works is to apply this pressure analysis method to identification of other two-phase flow patterns like entrainments and depositions in churn flow and annular flow.

References

[1] K. Mishima and M. Ishii, "Flow regime transition criteria for upward two-phase flow in vertical tubes," *Int. J. Heat Mass Transfer*, vol. 27, no. 5, pp. 723-737, 1983.

[2] M. Ishii and T. Hibiki, *Thermo-Fluid Dynamics of Two-Phase Flow*, Springer, NY, USA, pp. 3-9.

[3] S. W. Chen *et al*., "Experimental investigation and identification of the transition boundary of churn and annular flows using multi-range differential pressure and conductivity signals," *Applied Thermal Engineering*, vol. 114, pp. 1275-1286, 2016.

[4] B. J. Azzopardi and E. Wren, "What is entrainment in vertical two-phase churn flow?" *International Journal of Multiphase Flow*, vol. 30, no. 1, pp. 89-103, 2004.

[5] K. Wang *et al.*, "A physical model for huge wave movement in gas–liquid churn flow," *Chemical Engineering Science*, vol. 79, pp. 19-28, 2012.

[6] S. W. Chen, T. Hibiki, M. Ishii, M. Mori, and F. Watanabe, "Experimental study of adiabatic two-phase flow in an annular channel under low-frequency vibration," *Journal of Engineering for Gas Turbines and Power - Transactions of the ASME*, vol. 136, no. 3, pp. 032501:1-032501:11, 2014.

[7] S. W. Chen, Y. Liu, T. Hibiki, M. Ishii, Y. Yoshida, I. Kinoshita, M. Murase, and K. Mishima, "Experimental study of air-water two-phase flow in an 8x8 rod bundle under pool condition for one-dimensional drift-flux analysis," *International Journal of Heat and Fluid Flow*, vol. 33, no. 1, pp. 168–181, 2012.

[8] H. J. Lin *et al.*, *Transient Pressure Analysis and Visualization in Churn Flow*, Taichung, Taiwan, Dec. 1-2, 2017.

Hsiao-Jou Lin is a master student in the Department of Engineering and System Science at National Tsing Hua University (NTHU), Hsinchu, Taiwan. Her research interest focuses on identification of two-phase flow regimes.

Min-Song Lin is a Ph.D. candidate in the Institute of Nuclear Engineering and Science at National Tsing Hua University (NTHU), Hsinchu, Taiwan. His research interests include two-phase flow and reactor safety analysis.

Pei-Syuan Ruan is an undergraduate student in the Department of Engineering and System Science at National Tsing Hua University (NTHU), Hsinchu, Taiwan. Her research interests include two-phase flow, thermoelectric cooler and power generation.

Shao-Wen Chen is an Associate Professor in the Institute of Nuclear Engineering and Science at National Tsing Hua University (NTHU), Hsinchu, Taiwan. He received the Ph.D. degree from Purdue University, USA in 2012. His research interests include two-phase flow, boiling heat transfer, electronics cooling and reactor safety analysis.

Jin-Der Lee is a nuclear scientist at Nuclear Science and Technology Development Center in National Tsing Hua University, Hsinchu, Taiwan. He received his Ph.D. degree in Nuclear Engineering from National Tsing Hua University, Hsinchu, Taiwan, in 2000. His research interests include reactor safety, two-phase flow, boiling heat transfer, and stability analysis.

Jong-Rong Wang is an Adjunct Associate Professor in the Institute of Nuclear Engineering and Science at National Tsing Hua University (NTHU), Hsinchu, Taiwan. He received the Ph.D. degree from National Tsing Hua University (NTHU), Hsinchu, Taiwan. His research interests include nuclear power plant risk analysis, two-phase flow, and boiling heat transfer.